THE CONTACT MECHANISM OF AN ULTRASONIC MOTOR

Takashi Maeno Takayuki Tsukimoto Akira Miyake

Canon Inc. 3-30-2, Shimomaruko, Ota-ku
Tokyo, JAPAN

Abstract- This paper presents a new method to clarify the mechanical characteristics of an Ultrasonic Motor. We calculate the vibration mode of a stator by using the Finite Element Method (FEM,MSC/NASTRAN). The shape of the elliptic motion at the surface point of projections is obtained. We also measure the vibration mode of the projection by using electro optical displacement transducers made by Zimmer KG. Next, we calculate the dynamic contact condition of a stator and a rotor by using the FEM (JNIKE3D). The stick and slip at the contact surface of the stator and the rotor are taken into account. The displacement and the velocity of the stator projection and the rotor spring, the distribution of the stick and the slip area, the rotating speed of the rotor, and the friction loss at the contact area are all obtained when changing torque, pressure, friction factor, vibration amplitude of the stator, and stiffness of the rotor spring. The calculated rotor displacement and T-N curve correspond closely to the experimental ones. Furthermore, we measure internal loss of the stator, loss of the supporting felt, and internal loss of the rotor. The total loss of the motor obtained by adding the above losses and the calculated friction loss agree with the measured total loss. The calculated and the measured efficiency of the motor are also similar.

I. Introduction

An Ultrasonic Motor is a new type of actuator because of its high torque, low speed, simple shape, silence, and good controllability. Several types of Ultrasonic Motor have been proposed[1]-[4]. An Ultrasonic Motor of ring type developed by Canon [5],[6] for auto focusing lenses is one of then. Travelling wave is excited in a stator ring by piezoelectric ceramic. A press-contacted rotor is driven by the friction force between projections of a stator and a flange shaped spring of a rotor (Figure 1).

Since motor performance depends largely on the characteristics of the contact bettween a stator and a rotor, we need to understand the dynamic characteristics of the contact. In the recent years, some theoretical and experimental investigations have been undertaken. Ueha and Kurosawa calculated the T-N (Torque-Rotating Speed) curve and the efficiency of a motor by using the simple linear spring model of the rotor [7]. Yamabuchi and Kagawa solved the piezoelectric elastic structures using Finite Element Method (FEM) and proposed an equivalent electrical circuit [8]. However, they did not clarify the contact mechanism quantitatively because the nonlinearity of contact and the shear deformation near the contact area according to the stick and slip were not considered.

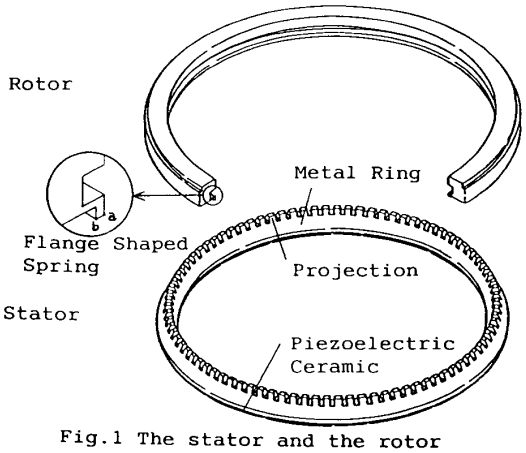

Fig.1 The stator and the rotor

In our research, we clarify the mechanical characteristics of a ring type Ultrasonic Motor. This paper is organized as follows. In SectionII, we calculate the vibration mode of a stator by using FEM (MSC/NASTRAN) to obtain the shape of elliptic motion at the surface point of projections. We also measure the vibration mode of projections by using the electro optical displacement transducer made by Zimmer KG. Accuracy of the simulation is confirmed by comparing the calculated result with the measured ones. In SectionIII, the effective method by using FEM (JNIKE3D) to clarify the motor contact characteristics is proposed. The simulated displacements, T-N curve, loss power, and efficiency are compared with the experimental ones.

II. Stator Viblation

In order to clarify the stator vibration mode, we analyze a stator characteristics. Figure 2 shows the FEM mesh model of a stator. Projections are placed to expand the velocity at the contact surface. One ninetieth of the stator along the circumferential direction is modeled. Natural frequency and natural mode are calculated by utilizing the cylindrical symmetry solution sequence of MSC/NASTRAN. Figure 3 shows the elliptic motion of some nodes when the seventh traveling wave is excited in a stator. It shows that the displacement on the theta direction is expanded at the projection. It also shows that the axis of the ellipse are not vertical at the edge of a stator projection due to an existence of projection. This result is compared with the vibration mode measured by the electro optical displacement transducer made by Zimmer KG. The calculated and the measured results were very close.

0-7803-0190-0/91$01.00 ©IEEE

Ⅲ. Contact between the Stator and the Rotor

3.1. Analysis Model

We calculate the dynamic contact behavior of a stator and a rotor by using a FEM code JNIKE3D. The stick and slip at the contact surface of a stator and a rotor are taken into account.

Mesh model is shown in Figure 4. It is known by experiment that the displacement of a stator ring due to a rotor contact is small enough. So only ninety projections of a stator are modeled to represent shear deformation. Bar elements are used to constrain the rotor ring on radial direction. Time step Δt is 5×10^{-7}sec. The step number is selected as 15 because the effect of initial state can be ignored when time step number is over 5. The elliptic motion of a stator is given from the first step at the bottom of stator projections as single point constraints on the r, θ and z direction. Rotor pressure is given at the top surface of a rotor ring from second step. Load torque is given at the inner side of a rotor as concentrate force on the θ direction from third step. The inertial force is ignored because that the natural frequency of a stator projection and a rotor spring are designed to be high enough compared with driving frequency (about 30kHz).

Super Computer S820 of Hitachi is used. CPU time to calculate one case is about 60 minutes (VPU 40 minutes).

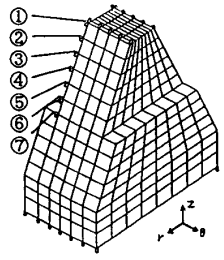

Fig.2 The finite element model of the stator

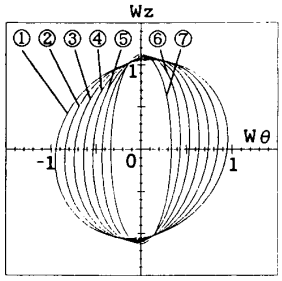

Fig.3 The elliptic motion of the stator projection

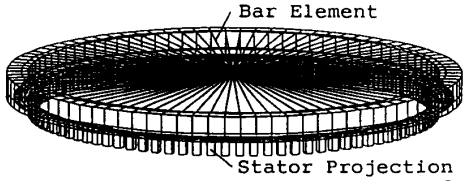

Fig.4 The analysis model for JNIKE/3D

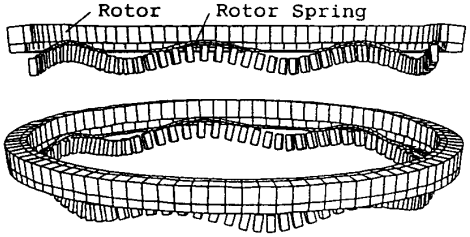

Fig.5 The deformation of the stator and the rotor

3.2. Comparison between the calculated and the measured result

Figure 5 shows the deformation of a stator and a rotor calculated by JNIKE3D. Rotor spring is bended and contact with stator projections at the top area of a stator traveling wave.

Figure 6(a) shows the displacement of stator projections and rotor spring on z direction when stator amplitude is 2(μmp-p), rotor load on the z direction is 14(N), and the load torque is zero. The cross axis is angle of the contact nodes. Sign (a) and (b) are location of the nodes as shown in Figure 1. Rotor deformation on z direction is about 0.82μm. Figure 6(b) shows the measured displacement of a stator projection and a rotor spring by the electro optical displacement transducer. The cross axis is time. The calculated and the measured deformation corresponded quantitatively.

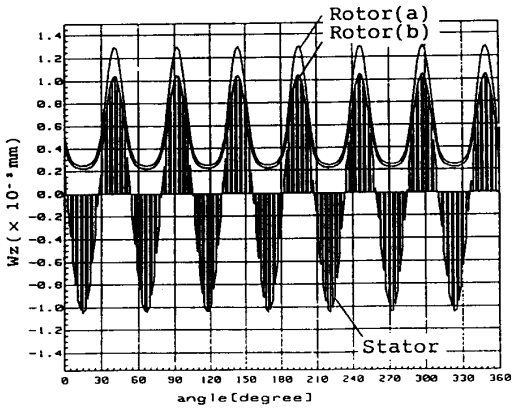

(a) Calculation

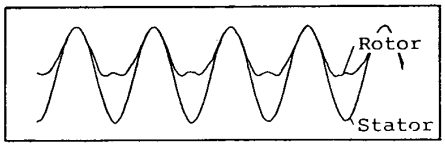

(b) Experiment

Fig.6 The displacement of the stator and the rotor on the z direction

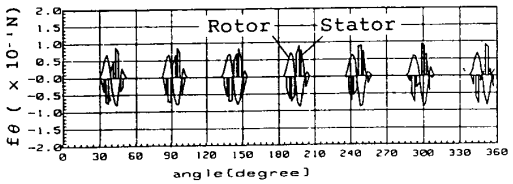

(a) T=0.00 N·m

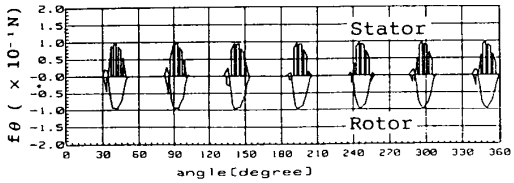

(b) T=0.05 N·m

Fig.7 The friction force between the stator and the rotor

Figure 7(a) and (b) shows the tangential force of a stator and a rotor when torque are zero and 0.05(N·m), respectively. When torque is zero, sum of the tangential force is zero. On the contrary, when torque is given, sum of that is not zero and balances with the torque.

Figure 8 shows the change of the tangential force at one node on a rotor spring. The cross axis is time. When a node on a rotor starts contacting with a stator, speed of a stator node is lower than that of a rotor node. So a stator and a rotor slip, and the tangential force f is proportional to the vertical force N at that point ($f = \mu d \cdot N$, μd:dynamic friction factor). When time passes and the speed of a stator node and a rotor node are equal, both of them stick and the tangential force f becomes smaller than maximumn steady friction force $\mu s \cdot N$ ($f < \mu s \cdot N$, μs : steady friction factor). After that, the speed of a stator node becomes higher and slip occours. When both speed are equal again, stick occours again. Later, a stator node becomes lower again and slips. Finally, a stator and a rotor voids.

This phenomenon is due to that the speed of a stator nodes periodically changes and a rotor shear deformation occours by the tangential force.

Figure 9 shows the calculated and the measured T-N curve. Steady friction coefficient μs is 0.48 and dynamic friction coefficient μd is 0.40. When the initial deformation of a stator and a rotor ($2 \cdot \cos(2 \cdot \theta)$ (μm), θ :circumferential angle) are considered in the calculation, T-N curve of the motor is close to the measured one.

Figure 10 shows the loss power of motor. The friction loss Wf is calculated from the result of FEM. As the velocity and the reflecting force are already obtained, Wf is calculated as follows,

$Wf = \Sigma (fi \times |vsi - vri|)$

fi : tangential force at the slipping node i
vsi : stator speed at the node i
vri : rotor speed at the node i
i : node on a stator (or a rotor)

The internal loss of a stator and a rotor, and loss of a supporting members are measured. The total loss of a motor obtained by adding an above losses and a calculated friction loss agree with a measured total loss. Accuracy of the calculation is confirmed.

Figure 11 shows the efficiency of motor. Calculated efficiency is obtained by above losses and an output power. The calculated and the measured efficiency are also similar.

Dynamic contact characteristics of an Ultrasonic Motor is clarified theoretically and experimentally as shown in this paper.

IV. Conclusion

The mechanical characteristics of a ring type Ultrasonic Motor is clarified quantitatively. First, we calculated the vibration mode of a stator by using FEM (MSC/NASTRAN) to obtain the shape of the elliptic motion at the surface point of the projection. We also measured the vibration mode of the projection by using an electro optical displacement transducer made by Zimmer KG. Accuracy of simulation is confirmed by comparing the calculated results with the measured ones. Next, an effective method to clarify the motor contact characteristics was proposed. FEM code JNIKE3D is used. The simulated displacements, T-N curve, loss power, and efficiency were in good agreement with the experimental ones.

From now on, the optimum shape of a ring type Ultrasonic Motor can be designed by utilizing this result and this simulation method.

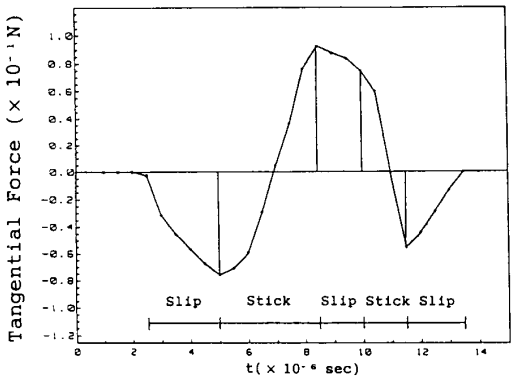

Fig.8 Tangential Force at One Point on The Rotor (P=10N,T=0,As=2 μ mp-p)

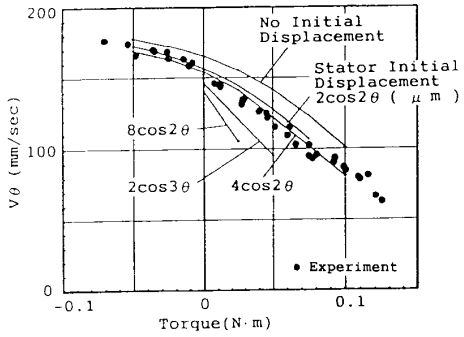

Fig.9 The T-N curve

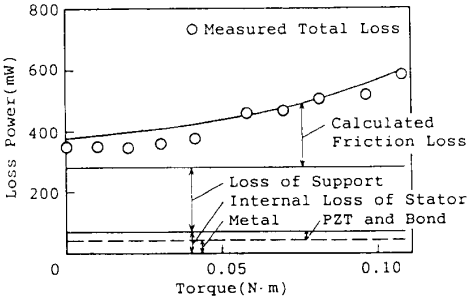

Fig.10 The loss of the motor

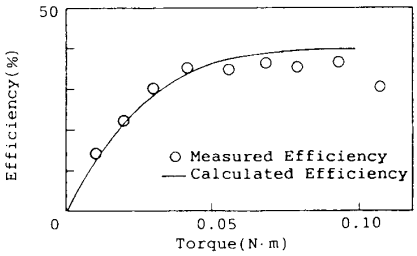

Fig.11 The efficiency

References

[1] S.Sashida,"Ultrasonic Motor",Jpn.J.Appl.Phy.,vol.54-6,1985,pp.589(in Japanese)

[2] A.Kumada,"A Piezoelectric Ultrasonic Motor",Jpn.J.Appl.Phy.,vol.24-2,1985,pp.739

[3] Y.Ise,"Ultrasonic Motor",J.Acoust.Soc.Jpn.,vol.54-6,1985,pp.589(in Japanese)

[4] M.Kurosawa et.al.,"An Ultrasonic Motor Using Bending Viblation of a Short Sylinder",IEEE Trans.UFFC,Sept.1989

[5] K.Hosoe,"An Application of Ultrasonic Motor to Automatic Focusing Lenzes",Tohoku Univ.Tsuuken Simposium,1989,pp.117(in Japanese)

[6] I.Okumura and H.Mukohjima,"A Structure of Ultrasonic Motor for Autofocus Lenses",Proceeding Motor-Con'87,1987,pp.75

[7] M.Kurosawa and S.Ueha,"Efficiency of Ultrasonic Motor Using Traveling Wave",J.Acoust.Soc.Jpn.,vol.44-1,1988,pp.40(in Japanese)

[8] T.Yamabuchi and Y.Kagawa,"Numerical Simulation of a Piezoelectric Ultrasonic Motor and Its Characteristics",Simulation,vol.8-3,1989,pp.69(in Japanese)

[9] T.Tsukimoto et.al.,"Measurement of Ring Type Ultrasonic Motor Vibration"JSAP,Vol.37,1990,pp.329(in Japanese)